weakly anisotropic upper mantle layer below 250 km depth is actively deforming by dislocation creep, and hence the top and bottom layers may be strongly coupled down to 400 km depth. Our predictions (that weak seismic anisotropy will develop in olivine-rich aggregates deforming by [001](*hk*0) slip in the deep upper mantle) challenge the two traditional interpretations for regions in the deep Earth of weak seismic anisotropy; (1) that they represent zones of poor deformation coherence at the seismic length scale, or (2) that the dominant deformation mechanism (for example, diffusion creep) in these regions does not produce CPO. Indeed, transition from dominant [100] to [001] slip at high pressure may explain the variation with depth of the anisotropy patterns of P and S waves, even if the entire upper mantle deforms coherently with a dominant horizontal shearing component (as expected in a convective system with large-scale plates at the surface, like the Earth's mantle). □

Received 11 August; accepted 30 November 2004; doi:10.1038/nature03266.

1. Montagner, J.-P. Seismic anisotropy of the Pacific Ocean inferred from long-period surface waves dispersion. *Phys. Earth Planet. Inter.* **38,** 28–50 (1985).
2. Cara, M. & Lévèque, J. L. Anisotropy of the asthenosphere: The higher mode data of the Pacific revisited. *Geophys. Res. Lett.* **15,** 205–208 (1988).
3. Nishimura, C. E. & Forsyth, D. W. The anisotropic structure of the upper mantle in the Pacific. *Geophys. J.* **96,** 203–230 (1989).
4. Montagner, J.-P. & Kennett, B. L. N. How to reconcile body-wave and normal-mode reference earth models. *Geophys. J. Int.* **125,** 229–248 (1996).
5. Karato, S.-I. On the Lehman discontinuity. *Geophys. Res. Lett.* **19,** 2255–2258 (1992).
6. Karato, S. I. & Rubie, D. C. Toward an experimental study of deep mantle rheology: a new multianvil sample assembly for deformation studies under high pressures and temperatures. *J. Geophys. Res.* **102,** 20111–20122 (1997).
7. Cordier, P. & Rubie, D. C. Plastic deformation of minerals under extreme pressure using a multi-anvil apparatus. *Mater. Sci. Eng. A* **309–310,** 38–43 (2001).
8. Durham, W. B., Weidner, D. J., Karato, S. I. & Wang, Y. in *Plastic Deformation of Minerals and Rocks* (eds Karato, S.-I. & Wenk, H.-R.) (American Mineralogical Society, Washington, 2002).
9. Couvy, H. *et al.* Shear deformation experiments of forsterite at 11 GPa – 1400 °C in the multianvil apparatus. *Eur. J. Mineral.* (in the press).
10. Tommasi, A. Forward modeling of the development of seismic anisotropy in the upper mantle. *Earth Planet. Sci. Lett.* **160,** 1–13 (1998).
11. Silver, P. G. Seismic anisotropy beneath the continents: Probing the depths of geology. *Annu. Rev. Earth Planet. Sci.* **24,** 385–432 (1996).
12. Ekstrom, G. & Diewonski, A. M. The unique anisotropy of the Pacific upper mantle. *Nature* **394,** 168–172 (1998).
13. Gung, Y., Panning, M. & Romanowicz, B. Global anisotropy and the thickness of continents. *Nature* **422,** 707–711 (2003).
14. Lévèque, J. J., Debayle, E. & Maupin, V. Anisotropy in the Indian Ocean upper mantle from Rayleigh and Love waveform inversion. *Geophys. J. Int.* **133,** 529–540 (1998).
15. Gaherty, J. B., Jordan, T. H. & Gee, L. S. Seismic structure of the upper mantle in the central Pacific corridor. *J. Geophys. Res.* **101,** 22291–22309 (1996).
16. Revenaugh, J. & Jordan, T. Mantle layering from ScS reverberations 3. The upper mantle. *J. Geophys. Res.* **96,** 19781–19810 (1991).
17. Li, L., Raterron, P., Weidner, D., Chen, J. & Vaughan, M. T. Stress measurements of deforming olivine at high pressure. *Phys. Earth Planet. Inter.* **143–144,** 357–367 (2004).
18. Li, L., Raterron, P., Weidner, D. & Chen, J. Olivine flow mechanisms at 8 GPa. *Phys. Earth Planet. Inter.* **138,** 113–129 (2003).
19. Ben Ismail, W. & Mainprice, D. An olivine fabric database: an overview of upper mantle fabrics and seismic anisotropy. *Tectonophysics* **296,** 145–158 (1998).
20. Ben Ismail, W., Barruol, G. & Mainprice, D. The Kaapvaal craton seismic anisotropy: petrophysical analyses of upper mantle kimberlite nodules. *Geophys. Res. Lett.* **28,** 2497–2500 (2001).
21. Vauchez, A., Dineur, F. & Rudnick, R. Microstructure, texture, and seismic anisotropy of the lithospheric mantle above a plume. Insights from the Labait volcano xenoliths. *Earth Planet. Sci. Lett.* (in the press).
22. Lebensohn, R. A. & Tomé, C. N. A self-consistent anisotropic approach for the simulation of plastic deformation and texture development of polycrystals: Application to zirconium alloys. *Acta Metall. Mater.* **41,** 2611–2624 (1993).
23. Wenk, H.-R., Bennet, K., Canova, G. R. & Molinari, A. Modelling plastic deformation of peridotite with the self-consistent theory. *J. Geophys. Res.* **96,** 8337–8349 (1991).
24. Tommasi, A., Mainprice, D., Canova, G. & Chastel, Y. Viscoplastic self-consistent and equilibrium-based modeling of olivine lattice preferred orientations. Implications for upper mantle seismic anisotropy. *J. Geophys. Res.* **105,** 7893–7908 (2000).
25. Abramson, E. H., Brown, M., Slutsky, L. J. & Zaug, J. The elastic constants of San Carlos olivine up to 17 GPa. *J. Geophys. Res.* **102,** 12252–12263 (1997).
26. Chai, M., Brown, J. M. & Slutsky, L. J. The elastic constants of a pyrope-grossular-almandine garnet up to 20 GPa. *Geophys. Res. Lett.* **24,** 523–526 (1997).
27. Collins, M. D. & Brown, J. M. Elasticity of an upper mantle clinopyroxene. *Phys. Chem. Miner.* **26,** 7–13 (1998).
28. Mainprice, D., Bascou, J., Cordier, P. & Tommasi, A. Crystal preferred orientations of garnet: Comparison between numerical simulations and electron back-scattered diffraction (EBSD) measurements in naturally deformed eclogites. *J. Struct. Geol.* **26,** 2089–2102 (2004).
29. Bascou, J., Tommasi, A. & Mainprice, D. Plastic deformation and development of clinopyroxene lattice preferred orientations in eclogites. *J. Struct. Geol.* **24,** 1357–1368 (2002).
30. Mainprice, D., Barruol, G. & Ben Ismaïl, W. in *Earth's Deep Interior: Mineral Physics and Tomography from the Atomic to the Global Scale* (eds Karato, S.-I., Forte, A. M., Liebermann, R. C., Masters, G. & Stixrude, L.) 237–264 (AGU, Washington DC, 2000).

Acknowledgements This Letter is dedicated to the memory of G. Canova, who introduced A.T. and D.M. to VPSC modelling. H.C. was supported by the Deutsche Forschungsgemeinschaft.

Competing interests statement The authors declare that they have no competing financial interests.

Correspondence and requests for materials should be addressed to D.M. (David.Mainprice@dstu.univ-montp2.fr).

Stratigraphic placement and age of modern humans from Kibish, Ethiopia

Ian McDougall[1], Francis H. Brown[2] & John G. Fleagle[3]

[1]*Research School of Earth Sciences, Australian National University, Canberra, ACT 0200, Australia*
[2]*Department of Geology and Geophysics, University of Utah, Salt Lake City, Utah 84112, USA*
[3]*Department of Anatomical Science, Stony Brook University, Stony Brook, New York 11794, USA*

In 1967 the Kibish Formation in southern Ethiopia yielded hominid cranial remains identified as early anatomically modern humans, assigned to *Homo sapiens*[1–4]. However, the provenance and age of the fossils have been much debated[5,6]. Here we confirm that the Omo I and Omo II hominid fossils are from similar stratigraphic levels in Member I of the Kibish Formation, despite the view that Omo I is more modern in appearance than Omo II[1–3]. $^{40}Ar/^{39}Ar$ ages on feldspar crystals from pumice clasts within a tuff in Member I below the hominid levels place an older limit of 198 ± 14 kyr (weighted mean age 196 ± 2 kyr) on the hominids. A younger age limit of 104 ± 7 kyr is provided by feldspars from pumice clasts in a Member III tuff. Geological evidence indicates rapid deposition of each member of the Kibish Formation. Isotopic ages on the Kibish Formation correspond to ages of Mediterranean sapropels, which reflect increased flow of the Nile River, and necessarily increased flow of the Omo River. Thus the $^{40}Ar/^{39}Ar$ age measurements, together with the sapropel correlations, indicate that the hominid fossils have an age close to the older limit. Our preferred estimate of the age of the Kibish hominids is 195 ± 5 kyr, making them the earliest well-dated anatomically modern humans yet described.

The principal outcrops of the Kibish Formation are along the Omo River where it skirts the Nkalabong Range (Fig. 1), with the highest outcrops close in elevation to that of the watershed between the Omo and the Nile rivers[7,8]. Former hydrographic links are apparent from Nilotic fauna in the Turkana Basin sequence[8–10].

The Kibish Formation (about 100 m thick) consists of flat-lying, tectonically undisturbed, unconsolidated sediments deposited mainly in deltaic environments over brief periods. It comprises the youngest exposed sedimentary sequence in the Omo Basin, and lies disconformably upon the Nkalabong Formation[11,12] or on the underlying Mursi Formation[12]. Strata are composed principally of claystone and siltstone, with subordinate fine sandstone, conglomerate and tuffs (Fig. 2).

Butzer *et al.*[13] and Butzer[14] divided the Kibish Formation into Members I to IV on the basis of disconformities with up to 30 m relief (Fig. 2). The members record discrete times of deposition

when the northern margin of Lake Turkana and the Omo delta lay about 100 km north of their current positions. As the higher lake levels reflect significantly higher precipitation in the region, such periods should be recognizable at least regionally, and perhaps globally.

Member I (26 m thick; Fig. 2) was deposited disconformably on the Nkalabong Formation in a deltaic environment. Small (less than 30 mm) rounded pumice clasts occur in an impure tuff in Member I, 7 m below the base of Member II. This tuff lies near, but probably slightly below, the levels from which Omo I and Omo II were derived. Glass shards from the tuff are very similar in composition to the glass from three pumice clasts enclosed in the tuff (Supplementary Table 1), indicating a common origin. Further, this composition is distinct from the glass composition of any other tuff in the Kibish Formation. Member II, about 28 m thick, was deposited on a topographic surface developed on Member I with at least 19 m of relief. Member II contains two discrete sequences, separated by an internal disconformity, designated Members IIa and IIb on Fig. 2. Member II was incised by as much as 25 m before the deposition of Member III[11,14], which begins with thin siltstone and claystone beds that drape topography. These beds, averaging about 3 cm thick, fine upward internally, and represent annual flooding. Thus, deposition of the lower part of Member III may record less than 1 kyr. A tuff 3.5–12 m thick, 18 m above the base of Member III, locally contains pumice clasts with alkali feldspar phenocrysts. Glass of the pumices normally differs compositionally from the glass of the tuff (Supplementary Table 1). However, one pumice sample yielded two contrasting sets of analyses: one corresponding to the tuff, the other to the dominant pumices. The youngest unit of the Kibish Formation, Member IV, was deposited on the underlying sediments after up to 30 m of dissection. Member IV comprises at most 21 m of strata deposited between about 9.5 and 3.3 kyr ago, on the basis of ^{14}C dating of mollusc shell[7,14,15].

Omo I was found at Kamoya's Hominid Site (KHS; 5° 24.15′ N, 35° 55.81′ E), which was identified from contemporary photographs, from evidence of the 1967 excavations and by additional hominid bone material conjoining the 1967 finds[16]. The hominid fossils were recovered from a siltstone 2.4 m below the base of Member II[14]. Thus, Omo I derives from near the top of Member I. Butzer *et al.*[13] reported a $^{230}Th/^{234}U$ date of 130 ± 5 kyr on *Etheria*

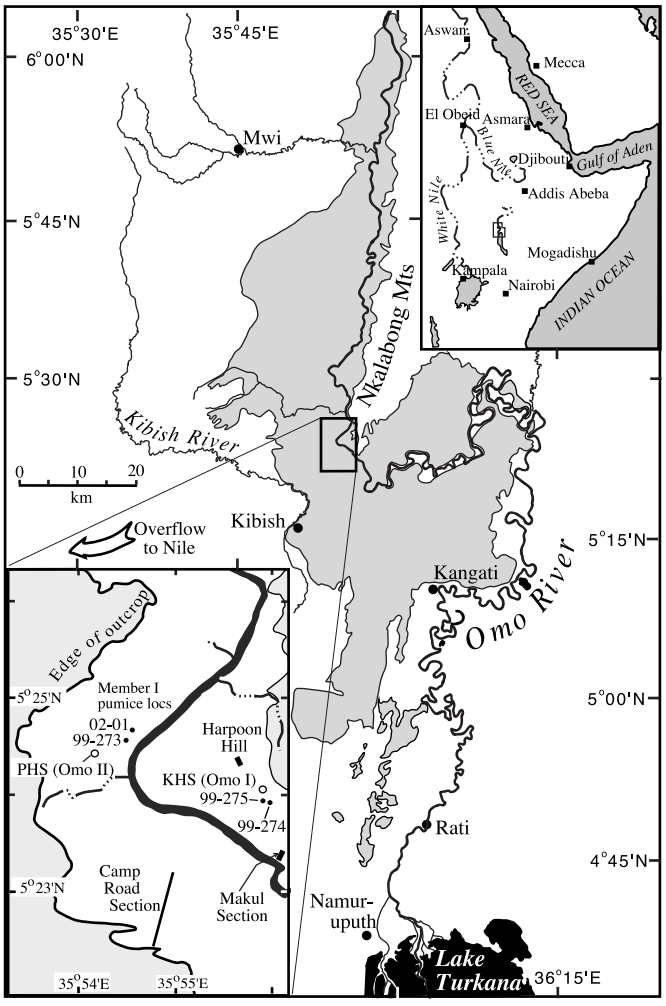

Figure 1 Map showing the distribution of the Kibish Formation (shaded) in the lower Omo Valley, southern Ethiopia, after Davidson[29]. Inset on lower left, locations of Omo I, Omo II, measured sections, and dated samples.

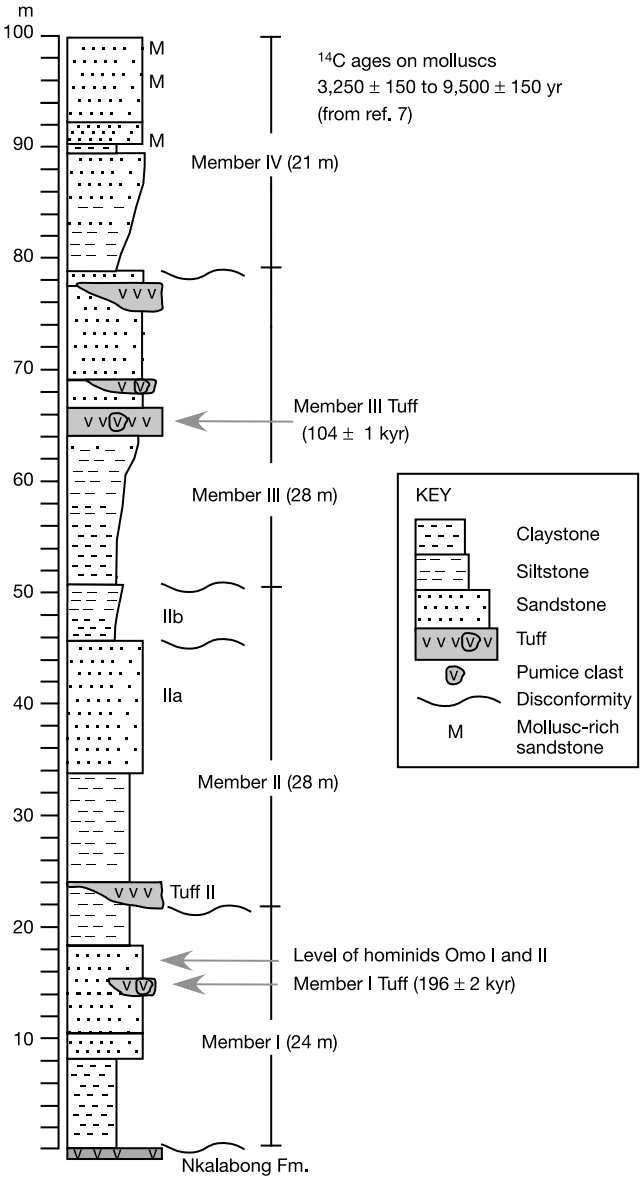

Figure 2 Composite stratigraphy of the Kibish Formation. Member I was measured near the type section at Makul; Member II was measured near Harpoon Hill, and Members III and IV were measured along Camp Road (see Fig. 1 for locations).

from essentially the same level as the hominid, but they and others have questioned the reliability of the age[5,6].

Omo II was found on the surface at PHS (Paul's Hominid Site), which Butzer[14] mapped about 2.6 km northwest of KHS. A map drawn at the time by Paul Abell (discoverer of Omo II), together with contemporary photographs of the site supplied by K.W. Butzer, have positively identified PHS at 5° 24.55′ N, 35° 54.07′ E, about 3.3 km west by north of KHS (Fig. 1). Although PHS was mislocated on the published map, Butzer's[14] stratigraphic description at the site is correct. The base of Member II lies about 3 m above the approximate level from which Omo II was recovered. The basal tuff of Member II is of unique composition, and correlates from KHS to PHS (Supplementary Table 1).

Ages on alkali feldspars separated from pumice clasts from tuffs in Members I and III reflect the time of their eruption, and provide maximum and minimum ages for the hominid fossils, respectively. $^{40}Ar/^{39}Ar$ results are summarized in Table 1, with details listed in Supplementary Tables 2–4.

The five pumice clasts measured from Member I yielded three different ages (Table 1), with at least the oldest age interpreted as evidence for reworking of that particular pumice clast. Nine analyses on 99-273A gave a mean age of 320 ± 19 kyr. Seven analyses on 99-273B yielded a mean age of 221 ± 13 kyr after rejecting one outlier (269 ± 18 kyr). Single feldspar crystals from 02-01B yielded a mean age of 195 ± 11 kyr ($n = 14$), forming a concordant data set after one rejection (333 ± 6 kyr). Multiple crystals ($n \leq 3$) were analysed in 12 of 16 measurements for 02-01A, and in 8 of 14 analyses for 02-01C ($n \leq 4$). No ages were rejected on 02-01A, whose mean age is 204 ± 15 kyr, or on 02-01C, whose mean age is 196 ± 15 kyr. It is probable that these latter three pumice clasts are products of the same volcanic eruption, as shown by their concordant ages and similar mean K/Ca ratios. When combined, all 44 analyses provide an arithmetic mean age of 198 ± 14 kyr and a weighted mean age of 195.8 ± 1.6 kyr. The mean age calculated for pumice 99-273B is statistically older than the ages determined on the three pumice clasts 02-01, so that 99-273B might also be a reworked pumice clast. Clearly, the age of deposition of a tuff must be younger than the youngest igneous component found within it. Thus, this tuffaceous level of Member I of the Kibish Formation was deposited after 196 kyr ago, on the basis of the mean age determined on the three 02-01 pumice clasts.

Feldspars from four pumice clasts from the Member III tuff were analysed. Two were *in situ* (99-275A, C), and two (99-274A, B) had weathered out of the same unit about 150 m farther east (Fig. 1). Ages on 99-275A range from 98.0 ± 7.7 kyr to 114.6 ± 4.3 kyr. Five single-crystal measurements have an arithmetic mean age of 105.5 ± 7.0 kyr, identical to five measurements on groups of two or three crystals (mean age 105.4 ± 2.7 kyr), indicating a homogeneous population. The overall mean age is 105.4 ± 5.0 kyr, with a weighted mean age of 106.0 ± 1.6 kyr. Eleven analyses on sample 99-275C yield a mean age of 107.5 ± 7.1 kyr and a weighted mean of 105.4 ± 1.8 kyr, after rejection of two outliers (142.1 ± 3.3 and 128.8 ± 8.3 kyr). Concordant results from 99-274A on seven single crystals and six pairs of crystals gave an overall arithmetic mean age of 98.1 ± 5.3 kyr. The companion clast 99-274B gave a mean age of 105.0 ± 8.3 kyr, after elimination of one outlier (Supplementary Table 4). Again these results reflect a single age population, as shown by the similar mean ages of the individual pumices, and the overlapping average K/Ca ratios. Combining all these results (except outliers), the overall arithmetic mean age is 103.7 ± 7.4 kyr ($n = 47$) and the weighted mean age is 103.7 ± 0.9 kyr. Thus, the depositional age must be equal to or younger than 104 kyr, providing evidence that Members I and II of the Kibish Formation are older than 104 kyr.

Each of the members of the Kibish Formation was deposited during intervals when Lake Turkana was at a much higher level than at present, and Member II has an internal disconformity. The upper part of Member I was being deposited at or after 196 kyr ago, and the upper part of Member III was being deposited at or after 104 kyr ago; ^{14}C ages on Member IV correspond to deposition between 9.5 and 3.3 kyr ago. These ages are remarkably similar to ages of Mediterranean sapropels S7, S4 and S1. Sapropels S1–S7 have the following estimated ages: 195 kyr (S7), 172 kyr (S6), 124 kyr (S5), 102 kyr (S4), 81 kyr (S3), 55 kyr (S2) and 8 kyr (S1)[17]. In many cases sapropels are related to a greatly increased flow of the Nile River into the Mediterranean Sea as a consequence of intensification of the African monsoon[18], recorded in more negative $\delta^{18}O$ in planktonic foraminifera. As the Omo River shares a divide with the Blue Nile and with tributaries of the White Nile, the Nile and the Omo must be affected similarly. As noted, deposition of each of the members of the Kibish Formation was probably very rapid. Thus, the close correspondence between the ages of Member I (196 kyr) and of sapropel S7 (195 kyr), of Member III (104 kyr) and of sapropel S4 (102 kyr), and of Member IV (3.3–9.5 kyr) and of sapropel S1 (8 kyr) is probably causally related. Sapropel S2 (55 kyr) is absent from or poorly represented in many Mediterranean sedimentary cores and has a very small $\delta^{18}O$ residual; thus, it is not surprising that no deposits of this age have been identified in the Kibish Formation. Sapropel S6, deposited during a European glacial period[19], might also be absent from the Kibish Formation, because it too has a small $\delta^{18}O$ anomaly. The two parts of Member II may be accommodated by sapropels S5 and S6, or they may correspond to the two phases identified in sapropel S5 (119–124 kyr), which are separated by 700–900 yr (ref. 20). This link between sapropel formation in the Mediterranean and very high levels of Lake Turkana is a particularly notable finding. In contrast, S3 is very well represented in many Mediterranean sedimentary cores and is

Table 1 **Summary of $^{40}Ar/^{39}Ar$ alkali feldspar laser fusion ages from pumice clasts in tuffs of the Kibish area, Turkana Basin, Ethiopia**

Sample no.	Tuff	Locality	Irradiation	*n*	*n* used	Simple mean age (kyr)	Weighted mean age (kyr)	Isochron age (kyr)	MSWD	$(^{40}Ar/^{36}Ar)_i$
Kibish Formation, Member III										
99-275A	Member III	0.4 km SSE of KHS	ANU58/L10	10	10	105.4 ± 5.0	106.0 ± 1.6	108.0 ± 3.1	1.03	292.2 ± 4.1
99-275C	Member III	0.4 km SSE of KHS	ANU58/L1	13	11	107.5 ± 7.1	105.4 ± 1.8	101.1 ± 8.4	2.04	303.6 ± 13.8
99-274A	Member III	0.5 km SE of KHS	ANU58/L6	13	13	98.1 ± 5.3	98.2 ± 1.1	97.4 ± 2.2	2.47	298.9 ± 6.8
99-274B	Member III	0.5 km SE of KHS	ANU58/L7	14	13	105.0 ± 8.3	109.6 ± 1.3	110.2 ± 4.4	3.27	292.9 ± 16.2
Kibish Formation, Member I, near Omo II site, just west of Omo River, Nakaa'kire, 5° 24.6′ N, 35° 54.5′ E										
99-273A	Member I	Nakaa'kire	ANU58/L3	9	9	319.8 ± 18.6	315.3 ± 3.6	318.2 ± 16.6	3.55	287.3 ± 41.5
99-273B	Member I	Nakaa'kire	ANU58/L4	8	7	220.8 ± 13.3	210.9 ± 2.1	209.6 ± 2.0	0.55	301.4 ± 3.1
02-01A	Member I	Nakaa'kire	ANU98/L9	16	16	204.2 ± 14.9	205.3 ± 2.2	194.1 ± 5.4	2.66	315.8 ± 7.3
02-01B	Member I	Nakaa'kire	ANU98/L10	15	14	194.7 ± 10.8	191.5 ± 1.9	184.9 ± 3.8	2.13	304.0 ± 3.5
02-01C	Member I	Nakaa'kire	ANU98/L3	14	14	195.6 ± 15.0	192.7 ± 2.3	192.5 ± 6.7	3.85	295.7 ± 5.8

^{40}K decay constant $\lambda = 5.543 \times 10^{-10}\,yr^{-1}$. Fluence monitor: Fish Canyon Tuff sanidine 92-176 of reference age 28.1 Myr. Samples 99-275A and 99-275C (laboratory sample numbers at ANU) = KIB99-47 (field sample number); 99-274A and 99-274B = KIB99-41; 99-273A and 99-273B = KIB99-19. Results with errors are means ± s.d. MSWD, mean square of weighted deviates.

therefore expected to be recorded in the Kibish Formation, but has not been recognized. Given the large expanse of the plain in the region underlain by the Kibish Formation, it is quite possible that deposits correlative with sapropel S3 are present but are not exposed in the immediate Kibish region that we have studied.

Our palaeontological and stratigraphic studies support the original report[14] that Omo I and Omo II are derived from comparable stratigraphic levels within Member I of the Kibish Formation despite their morphological differences[1–3,21,22]. Morphological diversity among fossil hominids from the Middle and Late Pleistocene of Africa is of major importance in understanding the tempo and mode of modern human origins[21,23].

$^{40}Ar/^{39}Ar$ dating of feldspars from tuffs in Member I and Member III of the Kibish Formation shows that its hominid fossils are younger than 195.8 ± 1.6 kyr and older than 103.7 ± 0.9 kyr. Direct isotopic dating of volcanic eruptions recorded in the Kibish Formation does not enable us to place narrower limits on the age. However, the suggested correlations of Member IIa and Member IIb with either the two identified phases of sapropel S5 or sapropels S6 and S5, respectively, indicate that deposition of Member I of the Kibish Formation occurred earlier than about 125 kyr ago or earlier than 172 kyr ago. The geological evidence for rapid deposition of Member I and the remarkably close correspondence of the isotopic ages on the youngest pumice clasts in the tuff of Member I at 196 kyr with the estimated age of sapropel S7 is regarded as strongly supporting the view that Member I was deposited close to 196 ± 2 kyr ago. On this basis we suggest that hominid fossils Omo I and Omo II are relatively securely dated to 195 ± 5 kyr old, somewhat older than the age of between 154 and 160 kyr assigned to the hominid fossils from Herto, Ethiopia[24], making Omo I and Omo II the oldest anatomically modern human fossils yet recovered. □

Methods

Age measurements

Alkali feldspar crystals were separated from pumice clasts and cleaned ultrasonically in 7% HF for 5–10 min to remove adhering volcanic glass and surface alteration. Although separations were performed on the coarsest crystals present, in several cases crystals were less than 1 mm, with masses less than 0.8 mg. In such cases several crystals were used for each analysis (see Supplementary Tables 2–4).

Samples were irradiated in facilities X33 or X34 of the High Flux Australian Reactor (Lucas Heights, Sydney, Australia) for 6 h as described in ref. 25. Cadmium shielding 0.2 mm thick was used to reduce the $(^{40}Ar/^{39}Ar)_K$ correction factor, which was measured by analysis of zero-aged synthetic potassium silicate glass co-irradiated with the unknowns. This correction is particularly important because of the young age of the samples, so interpolated values for each sample are given in the Supplementary Tables 2–4. The fluence monitor employed was sanidine 92-176, separated from the Fish Canyon Tuff, with a reference age of 28.1 Myr (ref. 26).

After irradiation, feldspar crystals were loaded into wells in a copper sample tray, installed in the vacuum system and baked overnight. Samples were fused with a focused argon-ion laser beam with up to 10 W of power. After purification of the gases released during fusion, the argon was analysed isotopically in a VG3600 mass spectrometer, using a Daly collector. The overall sensitivity of the system was about 2.5×10^{-17} mol mV^{-1}. Mass discrimination was monitored through regular measurements of atmospheric argon. The irradiation parameter, *J*, for each unknown was derived by interpolation from the measurements made on the fluence monitor crystals, with at least five analyses per level; the precision generally was in the range 0.3–0.75%, standard deviation of the population. Calcium correction factors[27] used in all calculations were $(^{36}Ar/^{37}Ar)_{Ca} = 3.49 \times 10^{-4}$ and $(^{39}Ar/^{37}Ar)_{Ca} = 7.86 \times 10^{-4}$.

Data handling

In calculating the arithmetic mean age for each pumice clast, any result more than two standard deviations from the initial mean of each sample was rejected iteratively until no further outliers were identified. No more than two measurements were rejected in any group of analyses, and no results were rejected for about half the groups. The error quoted in Table 1 is the standard deviation of the population, but because uncertainties on individual ages are variable, a weighted mean age and error is also given, weighting each age by the inverse of the variance. Differences in these mean ages are small (Table 1), but the error of the weighted mean age is usually much lower. In addition, data from each pumice clast, after exclusion of outliers, were plotted in an isotope correlation diagram ($^{36}Ar/^{40}Ar$ versus $^{39}Ar/^{40}Ar$), using the York[28] procedure. The derived ages are quite close to the mean ages (Table 1), and the calculated trapped argon composition generally has the atmospheric argon ratio of 295.5, within uncertainty.

Received 22 September; accepted 8 December 2004; doi:10.1038/nature03258.

1. Day, M. H. Omo human skeletal remains. *Nature* **222,** 1135–1138 (1969).
2. Day, M. H. & Stringer, C. B. in *Congrès International de Paléontologie Humaine I, Nice* Vol. 2, 814–846 (Colloque International du CNRS, 1982).
3. Day, M. H. & Stringer, C. B. Les restes crâniens d'Omo-Kibish et leur classification à l'intérieur du genre *Homo*. *Anthropologie* **95,** 573–594 (1991).
4. Day, M. H., Twist, M. H. C. & Ward, S. Les vestiges post-crâniens d'Omo I (Kibish). *Anthropologie* **95,** 595–610 (1991).
5. Howell, F. C. in *Evolution of African Mammals* (eds Maglio, V. J. & Cooke, H. B. S.) 154–248 (Harvard Univ. Press, Cambridge, Massachusetts, 1978).
6. Smith, F. H., Falsetti, A. B. & Donnelly, S. M. Modern human origins. *Yb Phys. Anthropol.* **32,** 35–68 (1989).
7. Butzer, K. W., Isaac, G. Ll., Richardson, J. L. & Washbourn-Kamau, C. Radiocarbon dating of East African lake levels. *Science* **175,** 1069–1076 (1972).
8. Fuchs, V. E. The geological history of the Lake Rudolf Basin, Kenya Colony. *Phil. Trans. R. Soc. Lond. B* **229,** 219–274 (1939).
9. Arambourg, C. *Mission Scientifique de l'Omo 1932–1933. Geologie–Anthropologie–Paleontologie* (Muséum National d'Histoire Naturelle, Paris, 1935–1947).
10. Butzer, K. W. The Lower Omo Basin: Geology, fauna and hominids of Plio-Pleistocene formations. *Naturwissenschaften* **58,** 7–16 (1971).
11. Butzer, K. W. in *Earliest Man and Environments in the Lake Rudolf Basin* (eds Coppens, Y., Howell, F. C., Isaac, G. Ll. & Leakey, R. E. F.) 12–23 (Univ. of Chicago Press, Chicago, 1976).
12. Butzer, K. W. & Thurber, D. L. Some late Cenozoic sedimentary formations of the Lower Omo Basin. *Nature* **222,** 1138–1143 (1969).
13. Butzer, K. W., Brown, F. H. & Thurber, D. L. Horizontal sediments of the lower Omo Valley: the Kibish Formation. *Quaternaria* **11,** 15–29 (1969).
14. Butzer, K. W. Geological interpretation of two Pleistocene hominid sites in the Lower Omo Basin. *Nature* **222,** 1133–1135 (1969).
15. Owen, R. B., Barthelme, J. W., Renaut, R. W. & Vincens, A. Palaeolimnology and archaeology of Holocene deposits north-east of Lake Turkana, Kenya. *Nature* **298,** 523–529 (1982).
16. Fleagle, J. *et al.* The Omo I partial skeleton from the Kibish Formation. *Am. J. Phys. Anthropol. Suppl.* **36,** 95 (2003).
17. Lourens, L. J. *et al.* Evaluation of the Plio-Pleistocene astronomical timescale. *Paleoceanography* **11,** 391–413 (1996).
18. Rossignol-Strick, M., Nesteroff, W., Olive, P. & Vergnaud-Grazzini, C. After the deluge: Mediterranean stagnation and sapropel formation. *Nature* **295,** 105–110 (1982).
19. Rossignol-Strick, M. & Paterne, M. A synthetic pollen record of the eastern Mediterrranean sapropels of the last 1 Ma: implications for the time-scale and formation of sapropels. *Mar. Geol.* **153,** 221–237 (1999).
20. Rohling, E. J. *et al.* African monsoon variability during the previous interglacial maximum. *Earth Planet. Sci. Lett.* **202,** 61–75 (2002).
21. Haile-Selassie, Y., Asfaw, B. & White, T. D. Hominid cranial remains from Upper Pleistocene deposits at Aduma, Middle Awash, Ethiopia. *Am. J. Phys. Anthropol.* **123,** 1–10 (2004).
22. Rightmire, G. P. in *The Origins of Modern Humans: A World Survey of the Fossil Evidence* (eds Smith, F. H. & Spencer, F.) 295–325 (Alan R. Liss, New York, 1984).
23. Howell, F. C. in *Origins of Anatomically Modern Humans* (eds Nitecki, M. H. & Nitecki, D. V.) 253–319 (Plenum, New York, 1994).
24. Clark, J. D. *et al.* Stratigraphic, chronological and behavioural contexts of Pleistocene *Homo sapiens* from Middle Awash, Ethiopia. *Nature* **423,** 747–752 (2003).
25. McDougall, I. & Feibel, C. S. Numerical age control for the Miocene–Pliocene succession at Lothagam, a hominoid-bearing sequence in the northern Kenya Rift. *J. Geol. Soc. Lond.* **156,** 731–745 (1999).
26. Spell, T. L. & McDougall, I. Characterization and calibration of $^{40}Ar/^{39}Ar$ dating standards. *Chem. Geol.* **198,** 189–211 (2003).
27. Spell, T. L., McDougall, I. & Doulgeris, A. P. The Cerro Toledo Rhyolite, Jemez Volcanic Field, New Mexico: $^{40}Ar/^{39}Ar$ geochronology of eruptions between two caldera-forming events. *Bull. Geol. Soc. Am.* **108,** 1549–1566 (1996).
28. York, D. Least squares fitting of a straight line with correlated errors. *Earth Planet. Sci. Lett.* **5,** 320–324 (1969).
29. Davidson, A. *The Omo River Project* (Bulletin 2, Ethiopian Institute of Geological Surveys, Addis Ababa, 1983).

Supplementary Information accompanies the paper on **www.nature.com/nature**.

Acknowledgements We thank J. Mya, R. Maier and X. Zhang for technical support for the geochronology; participants in the Kibish expeditions between 1999 and 2003, including Z. Assefa, J. Shea, S. Yirga, J. Trapani and especially C. Feibel, B. Passey and C. Fuller for their geological contributions; and R. Leakey, K. Butzer and especially P. Abell for providing us with information and documents about the 1967 expedition to the Kibish area. We thank the Government of Ethiopia, the Ministry of Youth, Sports and Culture, the Authority for Research and Conservation of Cultural Heritage, and the National Museum of Ethiopia for permission to study the Kibish Formation. Support was provided by the National Science Foundation, the Leakey Foundation, the National Geographic Society and the Australian National University. Neutron irradiations were facilitated by the Australian Institute of Nuclear Science and Engineering and the Australian Nuclear Science and Technology Organization.

Competing interests statement The authors declare that they have no competing financial interests.

Correspondence and requests for materials should be addressed to I.McD (ian.mcdougall@anu.edu.au).